

Timothy M. Barzyk* and John E. Frederick
Department of Geophysical Sciences, University of Chicago, Chicago, Illinois

1. INTRODUCTION

Metropolitan area surface climate can vary on scales as small as a single city block. Urban microclimates are discrete regions in the urban canopy layer (UCL) where radiative and weather variables hold to a consistent pattern. The UCL extends roughly from street-level to mean building height (Voogt and Oke, 2003). Urban microclimates may be as small as the footprint area of a single building or as large as 1-2 square kilometers. Collectively, individual urban microclimates produce the overall climate of a metropolitan area.

Variables influencing microclimate energy fluxes include the thermal, spatial and physical characteristics of underlying and vertical surfaces. Construction materials used in buildings and other urban landscape features alter surface radiation components, regional weather and atmospheric flows (Stemmers et al., 1998; Mills, 1997). Air and surface temperatures in urban environments are significantly different from those in non-urban settings characterized by soil and vegetative cover (Gallo, 1996)

Urban heat islands (UHIs) are indicated by positive temperature differentials between urban areas and their rural or suburban surroundings. Convective flow systems are also associated with UHIs (Haeger-Eugensson and Holmer, 1999; Morris and Simmonds, 2001). UHIs can be large or small, and of long or brief duration. They may define an annually-averaged temperature increment or consistently elevated temperatures at certain times of day.

Differences in measurement instruments and site characteristics can affect temperature readings. Thermometers might not have been interdependently calibrated or they could have been encased in non-equivalent weather shelters (Portman, 1993; Gallo, 2005). Monitoring stations can be situated in a variety of environments, from parks to private residences to urban rooftops, or at different latitudes or elevations (Gedzelman et al, 2003; Peterson, 2003). Large commercially

available datasets are frequently unadjusted to account for variations. UHI intensities may increase or decrease after corrections for non-equivalence (Peterson, 2003; Gallo, 2005).

Peterson (2003) analyzed a comprehensive mean monthly temperature dataset for 1989–91 for the contiguous United States. He corrected for heterogeneities and made adjustments for lack of standardization (site/instrument). His results show no statistically significant impact of urbanization on annual temperatures. He postulates that this may be a result of micro- and local-scale features, the impacts of which dominate over mesoscale UHIs. The present study attempts to document some of the effects of these types of features.

We first describe sites and instruments. Next, an energy budget model for artificial surfaces is presented. Energy fluxes from solar (Q_{SOL}) and terrestrial radiation (Q_{LW}), sensible heat transport (Q_{sens}), conduction ($Q_{CONDUCT}$) and evaporation (Q_{evap}) are given for different types of sites. Comparison of results from different types of sites aids in the description of characteristics of various urban microclimates.

2. METHODS

2.1 Site and Instrument Descriptions

Dual net radiometers and weather stations collected concurrent measurements from the roofs of two urban locations. Regional weather is assumed constant at both sites since they are in close proximity to each other (10 km), of similar elevation (~200 m), and within 5 km west of Lake Michigan.

The urban canyon site (Figure 1) is a 12-story building surrounded by tall structures, many over 30 stories. It is approximately one-third the height of the ~1.5 km² UCL that surrounds it. The urban canyon's rooftop is a white waterproof PVC-polymer with high albedo (0.36).

Tall structures do not surround the 5-story urban control site (Figure 2), which is 10 km south of the canyon. Its rooftop is black pitch covered with gray sedimentary pebbles (albedo of 0.23). The surrounding area is characterized by structures of similar height and composition, and

* Corresponding author address: Timothy M. Barzyk, Univ. of Chicago, Dept. of Geophysical Sciences, Chicago, IL 60637; e-mail: barzykt@uchicago.edu.

has more grassy open areas than the canyon area.



Fig. 1. Urban canyon site, aerial view. Dense shadows indicate a deep urban canopy layer. Photo courtesy of USGS.



FIG. 2. Urban control site, aerial view. Lack of shadows suggests shallow urban canopy; characterized by low-rise structures. Photo courtesy of USGS.

The Kipp and Zonen CNR-1 net radiometer has upward- and downward-facing sensors that measure energy received from the entire hemisphere (180 degrees field of view). Total spectral range measured is ~0.3 to 50 micrometers (μm), which includes both solar (0.3 - 3 μm) and terrestrial (5 - 50 μm) radiation, recorded in Watts per square meter. The upward-facing CM3 pyranometer measures incoming solar; the other, reflected. The ratio of reflected to incoming solar defines surface albedo. The

upward-facing CG3 pyrgeometer measures terrestrial radiation from the sky, the other from the surface.

The Davis Vantage Pro2 weather station includes a rain collector, temperature and humidity sensors, an anemometer and a solar radiation sensor. The temperature sensor has an accuracy of $\pm 0.5^\circ\text{C}$; humidity of $\pm 3\%$. The tipping bucket reads rainfall amounts in 0.2 mm increments. The anemometer measures wind speeds ranging from 0 to 274 km hr^{-1} . Dominant and high wind directions are also recorded. A fan-aspirated radiation shield reduces effects of solar radiation and rooftop heat on temperature readings.

The radiometers and weather stations were calibrated by running them side-by-side at the urban control site. When measurements were plotted against each other, the resulting slopes were ≈ 1 .

2.2 The Energy Balance of Urban Surfaces

An energy balance model provides a framework for interpreting the raw data. Five processes lead to energy exchanges between a surface and the atmosphere, described by fluxes expressed in Watts per square meter. Fluxes arise from: (a) absorption of solar energy at the surface, (b) absorption of incoming thermal radiant energy at the surface, (c) emission of thermal radiant energy at the surface, (d) exchange of sensible heat between surface and atmosphere, and (e) evaporative cooling, provided that liquid water is present.

Our regression model assumes the following surface energy balance:

$$0 = Q_{\text{LW}}(\text{up}) - Q_{\text{LW}}(\text{dn}) - Q_{\text{SOL}} + Q_{\text{SENS}} + Q_{\text{EVAP}} - Q_{\text{CONDUCT}}$$

It incorporates values of net radiation, surface and air temperatures and wind speed measured at ten-minute intervals from 4:00 AM on July 29 to 4:00 AM on August 5, 2005. From the derived coefficients, we infer time-dependent values for the flux of sensible heat and the difference between the fluxes for evaporative cooling and heat conduction. Q_{LW} and Q_{SOL} are measured values. Negative values indicate a warming effect.

The regression model explains 96.0% of the variance in net radiation observed at the control site and 83.7% at the canyon. All derived coefficients have high statistical significance, with the ratio of best estimate to standard error always exceeding 3.

3. RESULTS AND DISCUSSION

Average energy fluxes for the two sites are presented in Table 1. Negative values indicate a warming effect. Positive values indicate cooling. Q_{NET} is defined as total incoming minus total outgoing radiation. The figures represent 7 consecutive days of data that have been averaged into a 24-hr period, starting at 4:00 AM, with the x-axis representing the number of hours after 4:00 AM.

Flux Component	Value of Flux ($W m^{-2}$)	
	Control	Canyon
$-Q_{SOL}$	-244.8	-146.9
Q_{SOL} (reflected)	57.1	51.7
$-Q_{LW}$ (dn)	-389.8	-419.5
Q_{LW} (up)	484.2	465.5
$Q_{EVAP} - Q_{CONDUCT}$	28.6	27.1
Q_{SENS}	64.7	22.1
Q_{NET}	-93.3	-49.2

TABLE 1. Average energy fluxes for 7 consecutive 24-hr periods. Q_{NET} is total in minus total out.

Incoming solar (Figure 3) is strongly affected by the presence of tall structures. Diurnally averaged downward solar flux at the canyon is $\sim 100 W m^{-2}$ less than the control. Tall structures block the direct solar beam; so diffuse solar strikes the canyon in early morning and late afternoon. The canyon surface can reflect up to 36% of incoming solar because of its high albedo, as opposed to 23% at control, but when averaged diurnally, control reflects $\sim 6 W m^{-2}$ more.

Differences in solar heating are partially offset by enhanced downwelling thermal infrared radiation at the canyon, which is $\sim 30 W m^{-2}$ greater than the control throughout the 24-hr period (Figure 4). This suggests that tall structures are contributing to thermal storage of the canyon, and are a constant source of background thermal radiation. The control's underlying surface area emits $\sim 20 W m^{-2}$ more thermal radiation (diurnal average) due to its high surface temperatures (Figure 5).

The net effect of evaporative cooling and conduction ($Q_{EVAP} - Q_{CONDUCT}$) at both sites is between $27 - 29 W m^{-2}$, which is a cooling effect. Since no precipitation occurred during the recording period, this is likely the result of heat conduction downward into the cooler interior of the surface material.

Sensible heat transport out of the canyon is nearly a factor of three less than that of the control, due mainly to two processes. One is a smaller diurnal surface to air temperature

differential. The other is decreased wind speed due to wind blockage by tall structures. On average, winds are slower by $2.6 km hr^{-1}$ in the canyon (Table 2). Sensible heat transport is greater at the control, with a net cooling of $64.7 W m^{-2}$ compared to $22.1 W m^{-2}$ at the canyon.

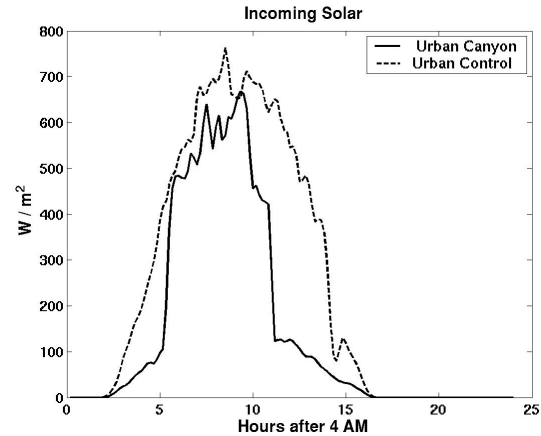


FIG. 3. Incoming solar radiation. 7 days averaged into a 24-hr period.

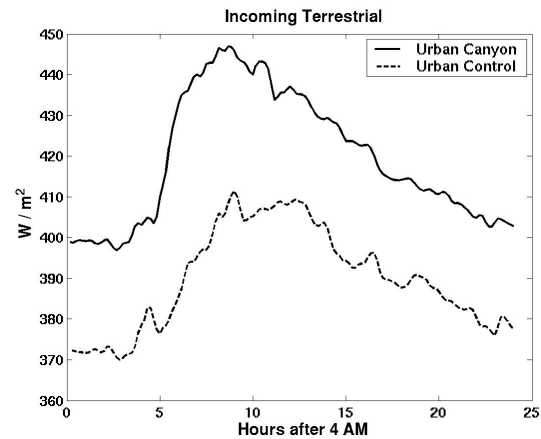


FIG. 4. Incoming terrestrial radiation (i.e., thermal infrared). 7 days averaged into a 24-hr period.

Figure 5 illustrates air and surface temperatures at the two locations. Air temperatures are greater in the canyon after 9:00 PM, denoting formation of a UHI. Intensity increases to maximum just before dawn the next day. Maximum air temperature difference (canyon - control) is $0.9^{\circ}C$ when 7 days are averaged into a 24-hr period. Maximum difference recorded was $1.7^{\circ}C$. Canyon surface temperatures are up to $12.4^{\circ}C$ cooler than control between 9:00 AM and 9:00 PM. Maximum recorded difference was a $19.9^{\circ}C$ cooler canyon

surface. In the evening, the canyon's slower cooling rate allowed its surface to become warmer than the control's.

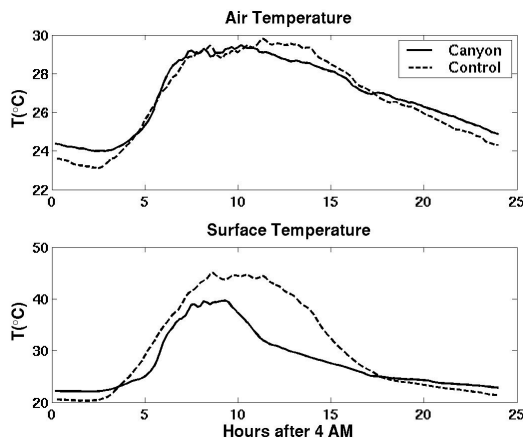


FIG. 5. Air and surface temperatures. 7 days averaged into a 24-hr period.

When air and surface temperatures are averaged over the entire 7-day period, there is little difference between the two sites (Table 2). The diurnal UHI is not evident; nor is a weekly-averaged UHI. Surface temperatures at the control are actually higher than those of the canyon.

	Control	Canyon
T _{SURF} (°C)	30.4	27.7
T _{AIR} (°C)	26.8	26.9
Wind Speed (km hr ⁻¹)	4.5	1.9

TABLE 2. Average air and surface temperatures and wind speed from 7 days of data.

4. CONCLUSIONS

Two urban microclimates were described on the basis of their model-derived energy fluxes and measured climate variables. Close proximity of the sites and inter-calibration of recording instruments are believed to have minimized extraneous effects in the measurements. Significant patterns and differences were found in solar and thermal radiation, air and surface temperatures, and wind speeds.

Tall structures at the urban canyon account for some of these differences. They block the direct solar beam, decreasing incoming solar radiation by $\sim 100 \text{ W m}^{-2}$ at the canyon. They increase incoming thermal by $\sim 30 \text{ W m}^{-2}$, which decreases air and surface cooling rates. Canyon walls slow the wind an average of 2.6 km hr^{-1} over the

control. Slow wind and a low surface to air temperature differential decrease sensible heat transport out of the canyon, which is one-third that of the control.

A UHI defines the state of air temperatures during evening and pre-dawn hours. The UHI forms each night around 9:00 PM, with its intensity increasing to maximum just before sunrise the next day. During the day, between 9:00 AM and 9:00 PM, air temperatures are similar at the two urban locations.

5. ACKNOWLEDGEMENTS

This research is supported by a grant from the Environmental Protection Agency. Aerial photos courtesy of United States Geological Survey (USGS).

6. REFERENCES

Gallo, K. P., 1996: The Influence of Land Use/Land Cover on Climatological Values of the Diurnal Temperature Range. *J. Climate*, **9**, 2941-2944.

Gallo, K. P., 2005: Evaluation of Temperature Differences for Paired Stations of the U.S. Climate Reference Network. *J. Climate*, **18**, 1629-1636.

Getzelman, S. D., Austin, S., Cermak, R., Stefano, N., Partridge, S., Quesenberry, S., Robinson, D. A., 2003: Mesoscale Aspects of the Urban Heat Island around New York City. *Theor. Appl. Climatol.*, **75**, 29-42.

Haeger-Eugensson, M. and Holmer, B., 1999: Advection Caused by the Urban Heat Island Circulation as a Regulating Factor on the Nocturnal Urban Heat Island. *Int. J. Climatol.*, **19**, 975-988.

Mills, G., 1997: The Radiative Effects of Building Groups on Single Structures. *En. Build.*, **25**, 51-61.

Morris, C. J. G., and Simmonds, I., 2001: Quantification of the Influences of Wind and Cloud on the Nocturnal Urban Heat Island of a Large City. *J. App. Met.*, **40**, 169-182.

Peterson, T. C., 2003: Assessment of Urban Versus Rural In Situ Surface Temperatures in the Contiguous United States: No Difference Found. *J. Climate*, **16**, 2941-2959.

Portman, D. A., 1993: Identifying and Correcting Urban Bias in Regional Time Series: Surface Temperature in China's Northern Plains. *J. Climate*, **6**, 2298-2308.

Stemmers, K., Baker, N., Crowther, J. D., Nikolopoulou, M., 1998: Radiation Absorption and Urban Texture. *Build. Res. & Inf.*, **26**, 103-112.

Voogt, J. A., and Oke, T. R., 2003: Thermal Remote Sensing of Urban Climates. *Rem. Sens. Env.*, **86**, 370-384.

This is a report of initial measurements and findings. Please contact the authors before citing or referencing this material.